PAPER • **OPEN ACCESS**

Double dielectric barrier (DBD) plasma-assisted deposition of chemical stabilized nanoparticles on polyamide 6,6 and polyester fabrics

To cite this article: A I Ribeiro *et al* 2017 *IOP Conf. Ser.: Mater. Sci. Eng.* **254** 102010

View the article online for updates and enhancements.

Related content

- Plasma-assisted deposition of microcapsule containing Aloe vera extract for cosmeto-textiles
S Nascimento do Carmo, A Zille and A P Souto
- Influence of the solid dielectric over the electric field from the ozone cell gap with double dielectric barrier
I Ganea
- Application of nanotechnology in antimicrobial finishing of biomedical textiles
Andrea Zille, Luís Almeida, Teresa Amorim et al.

This content was downloaded from IP address 193.136.11.91 on 20/11/2017 at 17:36

IOP Conf. Series: Materials Science and Engineering **254** (2017) 102010 doi:10.1088/1757-899X/254/10/102010

Double dielectric barrier (DBD) plasma-assisted deposition of chemical stabilized nanoparticles on polyamide 6,6 and polyester fabrics

A I Ribeiro[1], M Modic[2], U Cvelbar[2], G Dinescu[3], B Mitu[3], A Nikiforov[4], C Leys[4], I Kuchakova[4], M Vanneste[5], P Heyse[5], M De Vrieze[5], N Carneiro[1], A P Souto[1] and A Zille[1*]

[1]2C2T-Centro de Ciência e Tecnologia Têxtil, Minho University, Guimarães, Portugal
[2]Jožef Stefan Institute, Ljubljana, Slovenia
[3]National Institute for Lasers, Plasma and Radiation Physics, Măgurele, Romania
[4]Department of Applied Physics, Ghent University, Ghent, Belgium
[5]Centexbel Ghent, Technologiepark 7, 9052, Ghent, Belgium

E-mail: azille@2c2t.uminho.pt

Abstract. The development of new multifunctional textiles containing nanoparticles (NPs) has a special interest in several applications for pharmaceutical and medical products. Cu, Zn and Ag are the most promising antimicrobial NPs, exhibiting strong antibacterial activities. However, most of antimicrobial textiles coated with NPs are not able to perform a controlled release of NPs because of the high degree of aggregation. The aim of this study is to assess the effect of NPs stabilizers such as citrate, alginate and polyvinyl alcohol (PVA) in Cu, Zn and Ag NPs dispersions. The obtained dispersions were used to develop a new class of antibacterial NPs coatings onto polyamide 6,6 (PA66) and polyester fabrics (PES) by Double Dielectric Barrier (DBD) plasma discharge. Dynamic light scattering (DLS) was used to evaluate the best dispersing agent in terms of size, polydispersity index and zeta potential. Coating efficiency was evaluated by SEM, XPS and FTIR. The washing fastness of the coatings developed was also tested. The results show that the best dispersions were obtained using 2.5% of citrate for ZnO, 5% Alginate for Cu and 2.5% alginate for Ag NPs. SEM, XPS and FTIR analysis shows that DBD is an efficient deposition technique only for Ag and Cu NPs and that better perform in PA66 than PES fabric. The DBD deposition in air display similar results in term of NPS deposition of usually more efficient plasma jets using carrier gas such as N_2 and Ar.

1. Introduction

Medical textiles are used in a range of applications from bandages, dressings, suture and surgical clothing to implants such as scaffolds, stents and meshes.[1] Infections associated with these devices are responsible for at least 2-7% of post-operational complications increasing mortality and healthcare costs.[2] The typical strategies to prevent hospital-acquired infections rely either on inhibiting adhesion or on releasing biocidal compounds incorporated via novel physical and/or chemical methods.[3, 4] However, the increasing concern in the widespread use of biocides that might lead to bacterial resistance, has necessitated the development of new strategies.[5] Metals like Ag, Zn or Cu and their salts are well known for intrinsic antimicrobial property and the release of metal ions is

Content from this work may be used under the terms of the Creative Commons Attribution 3.0 licence. Any further distribution of this work must maintain attribution to the author(s) and the title of the work, journal citation and DOI.
Published under licence by IOP Publishing Ltd

believed to be the main reason for their antibacterial activity.[6] Recently, NPs as antimicrobial agents have increasingly been used in textile research due to their unique large surface-to-volume ratio, physicochemical properties and biological multi-target mechanism of action,[7] which may differ significantly from bulk material.[8] In order to suppress the potential hazard influence of the NPs on human bodies, it is important to fabricate antibacterial surfaces that firmly loading NPs and with precise local release of antibacterial ions.[9] One on the most important issue in the coating of metal or metal oxide NPs is their agglomeration in solution due to their high surface energy.[10] Stabilized NPs suspensions have been studied in regards of particle size, impurities, surfactants, polymers and capping ligands. Stabilizer such as starch, chitosan, alginate or citrate showed biocompatibility, low cost and environmental risks.[11, 12] One of most promising technologies for deposition of nanocomposite coating on industrial scale is the plasma-assisted polymerization and sputtering.[13, 14] However, these techniques have several limitations such as samples size, limited electrodes spacing, batch operation, low deposition rate and expensive vacuum systems that limit their application in textiles.[15] Atmospheric pressure plasma is an alternative and cost-competitive method to low-pressure plasma and wet chemical treatments, allowing continuous and uniform processing of fibres surfaces.[16] DBD is among the most effective cold atmospheric plasma sources[17] and have been attracting increasing interest for both surface activation and deposition of thin functional coatings.[18] In this project a new method for NPs DBD atmospheric plasma deposition in air using polyamide 6,6 and polyester fabrics as substrate was developed. The antimicrobial effect was provided by Cu, ZnO and Ag NPs stable dispersions using different stabilizers such as citrate, alginate and polyvinyl alcohol (PVA) were deposited on the fabrics and their antimicrobial efficiency assessed. The effect of DBD plasma developed in this work was also compared in term of deposition efficiency with two different atmospheric plasma jets configurations using carrier gases (N_2 and Ar).

2. Materials and Methods

2.1. Materials

Commercial pre-washed pure PA66 (warp 40, weft 18 threads cm^{-1}, areal density of 135 g m^{-2}) and PES (warp 56, weft 30 threads cm^{-1}, areal density of 100 g m^{-2}) woven fabrics were used in this study. All the other reagents were purchased from Sigma–Aldrich, St. Louis, MO, USA.

2.2. Atmospheric DBD Plasma in air

DBD plasma treatment was performed in a semi-industrial prototype (Softal GmbH/University of Minho) working at RT and atmospheric pressure in air, using a metal electrode coated with ceramic and counter electrodes coated with silicon with a gap distance fixed at 3 mm and producing the discharge at high voltage 10 kV and low frequency 40 kHz. The optimized fixed parameters of 1 kW of power and velocity of 5 m min^{-1} was used. The dosage (D) applied was 2.5 kW m^2 min^{-1}.

2.3. Atmospheric DC plasma jet in N_2

AgNPs were deposited using an atmospheric pressure direct current (DC) plasma jet using N_2 as carrier gas. The plasma is generated between a pin and a mesh electrode placed in a quartz tube. The plasma was generated with a fixed power at 22.5 W and a total flow rate at 8 standard liter per minute (SLM). The substrate was placed at 10 mm from the nozzle, where the gas temperature is 37 ºC.

2.4. Atmospheric RF DBE plasma jet in Ar

DBE plasma coaxial design consists in a central hollow metallic RF electrode, surrounded by an internal ceramic insulator and an external grounded metallic electrode envelope. The Ar flowed (2500 sccm) along the gap delimited between the central electrode and the ceramic insulator. In the hollow electrode, a mixture of Ar, HDMSO and NPs was atomized (900 sccm). The discharge is generated in the space between the central electrode and the nozzle using a 13.56 MHz (15 W) RF power supply.

2.5. Preparation and application of NPs dispersions

Ag, Cu or ZnO NPs water dispersions (10μgmL^{-1}) were prepared using alginate, citrate and PVA in different concentrations (1, 2.5 and 5 %wt) in a ultrasonic bath for 30 min followed by an ultrasonic tip for more 30 min. Fabric samples (10x10 cm) were immerged in the NPs suspension at RT with magnetic agitation and ultrasonic tip at 80% of intensity for 5 min. For DC plasma jet the coating was by dipping. For DBE plasma jet the deposition of NPs was performed directly in the plasma jet.

2.6. Dynamic light scattering (DLS) analysis

The NPs size distribution, polydispersity index and zeta potential were measured by dynamic light scattering (DLS) and electrophoretic light scattering (ELS) using a Zeta Sizer-Nano (Malvern Instruments). Data was collected after 30 scans at a constant temperature of 25 ± 1ºC. Zeta potentials were measured in solution at a moderate electrolytic concentration.

2.7. *Fourier transform infrared spectroscopy (FTIR)*

A Nicolet Avatar 360 FTIR spectrophotometer (Madison, USA) with an attenuated total reflectance accessory (ATR) was used to record the IR spectra of the fabric samples. The spectra were collected in the region of 4000–650 cm^{-1} and at a resolution of 4 cm^{-1} with 45 scans at room temperature.

2.8. Scanning electron microscopy (SEM)

SEM analyses were carried out with an ultra-high resolution Field Emission Gun Scanning Electron Microscope (FEG-SEM), NOVA 2000 Nano, SEM, FEI Company. Secondary electron images were performed with an acceleration voltage between 5 and 10 kV. Backscattering Electron Images were made with an acceleration voltage of 15 kV. Samples were covered with Au–Pd (80-20 wt%).

2.9. X-ray photoelectron spectroscopy (XPS)

Samples were excited with X-rays over a 400 μm spot area with a monochromatic Al Kα1,2 radiation at 1486.6 eV in a TFA-XPS Physical Electronics (Chanhassen, USA). The photoelectrons were detected with a hemispherical analyzer at an angle of 45° with respect to the normal to the sample surface. Survey-scan spectra were made at pass energy of 187.85 eV with a 0.4 eV energy step.

2.10. Washing fastness

The washing fastness was evaluated after performing 5 washing cycles according to EN ISO 15797 in a laboratory-dyeing machine (Haiba) at 75°, 40 rpm, for 15 min with 0,1gL^{-1} nonionic surfactant, in liquor bath ration 1:30.

3. Results and Discussion

To solve the instability and aggregation problems of Ag, Cu and ZnO NPs suspensions (10 ppm) of citrate, alginate and PVA using water and ethanol as control were prepared in different concentrations (1, 2.5 and 5 wt%) using an ultrasonic bath. Table 1 shows the best results obtained for each NP compared to water as control. Ethanol and PVA were disregarded due to the highest instability and lowest ζ potential, respectively.

Table 1. DLS and zeta potential measurements of suspensions tested

	ZnO NPs		**Cu NPs**		**Ag NPs**	
	Water	Citrate 2.5%	Water	Alginate 5%	Water	Alginate 2.5%
ζ (mV)	-17.3±4.2	-38.7±2.5	-0.2±0.3	-32.3±2.7	-19.7±0.8	-28.6±1.4
Size (dnm)	172.6±4.8	176.2±2.3	468.2±22.8	774.8±173.7	239.9±17.6	184.9±8.3

Zeta potential (ζ) is the measure of the electrical potential at the interface between the moving and the stationary solvent layers around colloidal particles and it provides useful information about NPs stability and their ability to interact with a substrate [19]. A suspension that exhibits a ζ potential less

than ± 30 mV is considered unstable and will result in rapid NPs deposition or aggregation [20]. Table 1 shows that all the used NPs possess a high negative ζ potential when a stabilizer is considered instead of water. With the only case of Cu all the other NPs display lower size and polydispersivity (PDI) in presence of the used stabilizers. Despite the higher ζ potential, Cu NPs increase in size and PDI probably due to their instability in an oxidative environment and because ζ potential of colloid particles also depends on the ionic strength and dielectric constant of the medium [21]. The SEM images (Figure 1) of the deposited NPs in plasma treated PA66 and PES show a good widespread load of NPs at the expected size but a high aggregation and a not uniform distribution as previously observed at this low NPs concentration (10 ppm) [22]. The stabilized NPs tend to aggregate in clusters on the surface of the DBD-treated PA66 fibers due to the chemical changes on surfaces induced by plasma treatment [23]. All the NPs deposited on the PA66 fabrics (Figure 1 a, c, e) display a higher load than PES fabrics (Figure 1 b, d, f). In the case of ZnO NPs the deposition efficiency is very low in PA66 and almost none in PES fabric. This behavior is probably caused by the similar charges of the metal oxide NPs with the oxygen species on the fabric surface. Usually, to immobilize ZnO in a plasma oxidized surface, it is necessary to provide zinc in the ionic form. In this fashion, Zn^{2+} is able to interact with the negative charges onto the fabric surface and thus creating the oxidized form ZnO.[24] After 5 washing cycles at 75 ºC some Ag and Cu NPs are still detected onto the surface of both PA66 and PES. However, no ZnO NPs can be detected in the SEM analysis (data not shown).

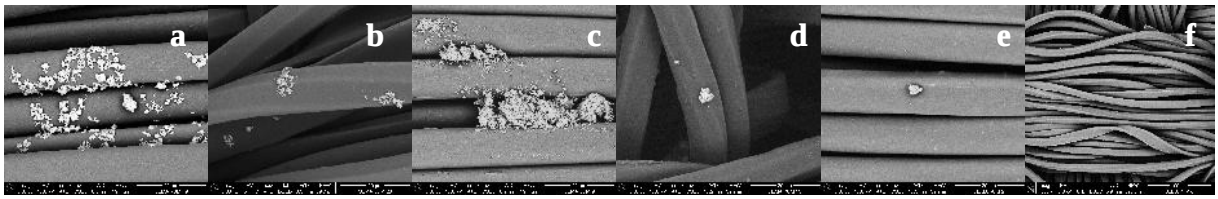


Figure 1. SEM of Ag (a, b), Cu (c, d) and ZnO NPs (e, f) onto PA66 and PES fabrics, respectively.

The FTIR analysis for PES and PA66 showed similar results. For convenience only the data of PA66 (Figure 2-c) are presented. The ATR-FTIR spectrum of plasma treated PA66 sample shows the typical bands of PA66 at 3290, 2930 and 2850 cm^{-1} which may be attributed to N–H stretching vibrations and to the CH_2 asymmetric and symmetric stretching vibrations, respectively [25]. The amide I absorption band at 1630 cm^{-1} is assigned to the amide carbonyl C=O stretching vibrations. The amide II band at 1530 cm^{-1} may be attributed to N–H bending motion. The band at 680 cm^{-1} is attributed to the bending of O=C–N group [26]. The shoulder at 720 cm^{-1} is attributed to the in-plane N-H deformation vibration of the hydrogen-bonded secondary amide. Compared to the untreated sample the plasma treatment did not introduce new peaks but displays a significant increase in the intensity of the C=O stretching band as well as of the bending band of the O=C–N group. This may be an indication of plasma-promoted oxygen addition on the fiber surface. The addition of NPs onto the fabrics surface after plasma treatment shows the appearance of low-intensity peaks in the range between 1700-1750 cm^{-1} and 3500–4000 cm^{-1} attributed to carboxylic acids (-COOH) and hydroxyl groups (-OH), respectively.[27] These peaks suggest the interaction of NPs in their oxidized form with the plasma-produced oxygen species onto the PA66 surface. The XPS analysis confirms the plasma modification on the fabrics. It is clear that the plasma treatment is able to increase the concentration of polar groups near the surface of the fabric mainly by the incorporation of oxygen atoms from atmospheric air. Figure 2-a shows the deconvolution of the C1s core level of the plasma treated PES. The peak at 284.6 and 285.6 eV can be attributed to aliphatic carbon atoms of the PES structure (–CH_2–CH_2–) and the peak at 286.6 eV represents the carbon atoms neighboring the single bonded oxygen (–C-O–) and that of at 288.7eV is assigned to the carboxylic groups (O=C–O–) [28]. Compared to the untreated sample the results indicate that DBD treatment led to a significant increase in the content of C=O and O–C=O groups on the surface of PES [29]. Similar results were obtained for PA66 (data not shown). After the Cu NPs deposition, the C1s deconvolution shows the presence of

a new peaks at 289.6 eV (Figure 2-b). This peak could be attribute to the interaction of the oxidized form of Cu with the plasma-induced oxygen species onto the PES surface. This energetic peak is usually associate to the presence of carboxylic group not influenced by the mesomeric effect induced by the benzene ring in PES [30].

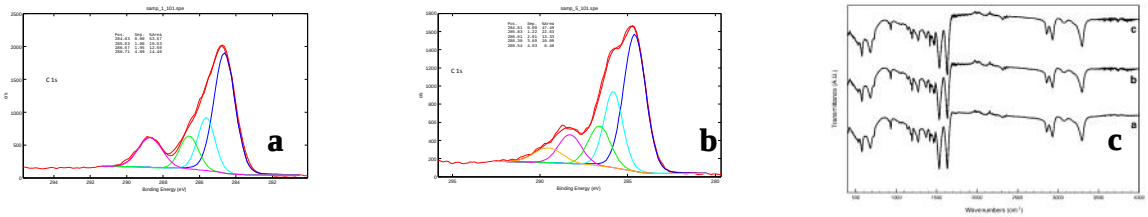


Figure 2. High-resolution XPS deconvoluted spectra of the C1s envelope of plasma treated PES without (up) and with Cu NPs (down). FTIR spectra of the plasma treated PA66 without NPs (a) and with coated Ag (b) and Cu (c).

In order to assess the efficacy of the DBD plasma treatment, two different plasma jet techniques were performed and compared to the DBD in term of deposited NPs by SEM analysis. A DC plasma jet using N_2 as carrier gas and a RF DBE plasma jet using Ar as carrier gas were used to modify a PES fabric and deposit Ag NPs onto its surface (Figure 3). For similar NPs concentrations, the DC plasma jet using N_2 shows similar results including a high degree of NPs aggregation (Figure 3-A) while, the RF plasma jet using Ar display a widespread distribution and higher concentration of NPs onto the fabric surface. Overall, the DBD plasma technique showed comparable results despite the absence of a carrier gas and the used lower energies.

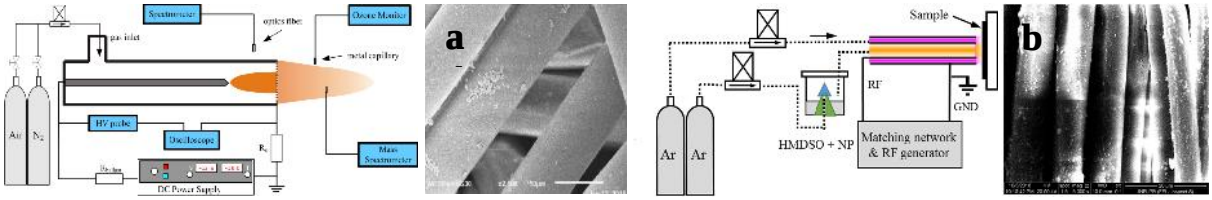


Figure 3. Schematics of the N_2 DC (A) and Ar RF DBE (B) plasma jets and respective SEM analysis of deposited Ag NPs onto PES fabrics.

4. Conclusion

The NPs were successfully stabilized improving their deposition onto PA66 and PES fabric surfaces. However, despite the improving in ζ potentials the obtained NPs still show a moderate degree of aggregation. FTIR, XPS and SEM confirm plasma modification on the fabric as well as the successful deposition of Ag and Cu NPs. ZnO NPs show very low deposition efficiency due to the ionic repulsive interactions with the oxygen species on the DBD plasma treated surface. The comparison of the DBD plasma with two different atmospheric plasma jets using N_2 and Ar as carrier gases showed similar deposition efficacy despite the RF DBE jet plasma using Ar presents higher load and uniform NPs distribution. Preliminary, antimicrobial tests in PES (data not shown) show that all the NPs have an antimicrobial effect but Cu and Zn show activity only in S. aureus and Ag only in E.coli. Overall, the DBD atmospheric plasma treatment in air allows high level of NPs deposition and fixation on PA66 and PES fibers at lower temperatures and processing times, without the need of a carrier gas.

Acknowledgements

This work was funded by Portuguese Foundation for Science and Technology FCT/MCTES (PIDDAC) and co-financed by European funds (FEDER) through the PT2020 program,

research project M-ERA-NET/0006/2014 and COMPETE program through FCT within the scope of the project POCI-01-0145-FEDER-007136 and UID/CTM/00264.

References

[1] Radetić M 2012 *J. Mater. Sci.* **48** 95-107
[2] Deng X, Leys C, Vujosevic D, Vuksanovic V, Cvelbar U, De Geyter N, Morent R and Nikiforov A 2014 *Plasma Processes Polym.* **11** 921-30
[3] Banerjee I, Pangule R C and Kane R S 2011 *Adv Mater* **23** 690-718
[4] Lo J, Lange D and Chew B 2014 *Antibiotics* **3** 87-97
[5] Hasan J, Crawford R J and Lvanova E P 2013 *Trends Biotechnol.* **31** 31-40
[6] Hajipour M J, Fromm K M, Akbar Ashkarran A, Jimenez de Aberasturi D, Larramendi I R d, Rojo T, Serpooshan V, Parak W J and Mahmoudi M 2012 *Trends Biotechnol.* **30** 499-511
[7] Chernousova S and Epple M 2013 *Angew. Chem. Int. Ed.* **52** 1636-53
[8] Zille A, Almeida L, Amorim T, Carneiro N, Esteves M F, Silva C J and Souto A P 2014 *Mater. Res. Express* **1** 032003
[9] Zille A, Fernandes M M, Francesko A, Tzanov T, Fernandes M, Oliveira F R, Almeida L, Amorim T, Carneiro N, Esteves M F and Souto A P 2015 *ACS Appl. Mater. Interfaces* **7** 13731-44
[10] Sager T M, Wolfarth M, Leonard S S, Morris A M, Porter D W, Castranova V and Holian A 2016 *Inhalation Toxicol.* **28** 686-97
[11] Afshinnia K, Sikder M, Cai B and Baalousha M 2017 *J. Colloid Interface Sci.* **487** 192-200
[12] Sharma S, Sanpui P, Chattopadhyay A and Ghosh S S 2012 *RSC Advances* **2** 5837-43
[13] Ivanova A A, Surmenev R A, Surmeneva M A, Mukhametkaliyev T, Loza K, Prymak O and Epple M 2015 *Appl. Surf. Sci.* **329** 212-8
[14] Alissawi N, Peter T, Strunskus T, Ebbert C, Grundmeier G, Faupel F 2013 *J. Nanopart. Res.* **15**
[15] Pappas D 2011 *J. Vac. Sci. Technol. A* **29** 020801
[16] Jia C X, Chen P, Liu W, Li B and Wang Q A 2011 *Appl. Surf. Sci.* **257** 4165-70
[17] Radić N, Obradović B M, Kostić M, Dojčinović B, Kuraica M M and Černák M 2012 *Surf. Coat. Technol.* **206** 5006-11
[18] Zille A, Oliveira F R and Souto A P 2015 *Plasma Processes Polym.* **12** 98-131
[19] Alvarez-Puebla R A, Arceo E, Goulet P J G, Garrido J J and Aroca R F 2005 *J. Phys. Chem. B* **109** 3787-92
[20] El Badawy A M, Luxton T P, Silva R G, Scheckel K G, Suidan M T and Tolaymat T M 2010 *Environ. Sci. Technol.* **44** 1260-6
[21] Sarkar A, Kapoor S and Mukherjee T 2005 *J. Phys. Chem. B* **109** 7698-704
[22] Radetic M, Ilic V, Vodnik V, Dimitrijevic S, Jovancic P, Saponjic Z and Nedeljkovic J M 2008 *Polym. Adv. Technol.* **19** 1816-21
[23] Montazer M, Shamei A and Alimohammadi F 2012 *Prog. Org. Coat.* **74** 270-6
[24] Paisoonsin S, Pornsunthorntawee O and Rujiravanit R 2013 *Appl. Surf. Sci.* **273** 824-35
[25] Charles J, Ramkumaar G R, Azhagiri S and Gunasekaran S 2009 *E-J. Chem.* **6** 23-33
[26] Kale K H and Palaskar S S 2012 *J. Text. Inst.* **103** 1088-98
[27] Su F and Lu C 2007 *Journal of Environmental Science and Health, Part A* **42** 1543-52
[28] Gupta B, Hilborn J, Hollenstein C, Plummer C J G, Houriet R and Xanthopoulos N 2000 *J. Appl. Polym. Sci.* **78** 1083-91
[29] Ilić V, Šaponjić Z, Vodnik V, Molina R, Dimitrijević S, Jovančić P, Nedeljković J and Radetić M 2009 *J. Mater. Sci.* **44** 3983-90
[30] Idage S B, Dumbre M D and Singh R 2000 *Proceedings of Recent Advances in Polymers and Composites.*: Allied Publishers) p 703